MULTISTATIC MATCHED-ILLUMINATION WAVEFORM DESIGN FOR DETECTION AND IDENTIFICATION OF INDOOR TARGETS BEHIND WALLS

Fauzia Ahmad and Moeness G. Amin

Radar Imaging Lab, Center for Advanced Communications, Villanova University
800 E. Lancaster Ave, Villanova, PA 19085, USA.
phone: + (1) 610 519 8919, fax: + (1) 610 519 6118, email: {fauzia.ahmad, moeness.amin}@villanova.edu

ABSTRACT

We present the matched illumination waveform design for improved target detection and identity discrimination in through-the-wall radar imaging and sensing applications. We consider a multistatic radar system for detection and identification of stationary targets with known impulse responses behind walls. The stationary and slowly moving nature of typical indoor targets relaxes the orthogonality requirement on the waveforms, thereby allowing sequential transmissions from each transmitter with simultaneous reception at multiple receivers. Numerical electromagnetic modeling is used to provide the impulse responses of a human and a wooden table for different target orientations and at various incident and reflection angles. Simulation results, depicting an improvement in performance of the multistatic radar as compared to monostatic operation, are provided.

1. INTRODUCTION

Utilization of target signature for design of transmission waveforms for optimum detection and classification has been recently investigated in many applications of radar, such as air-to-air and air-to-ground radar systems [1]-[3]. However, it has not been utilized in the context of urban sensing and through-the-wall radar imaging (TWRI). This new emerging field of research and development involves the process of remotely detecting, classifying, and locating targets inside buildings or other structures [4]. In addition to surveillance and reconnaissance in urban environments, this technology can also be used in rescue missions, searching for fire, earthquakes, and avalanche victims and survivors, and behind-the-wall detection and surveillance of suspected criminals and outlaws [5]-[6]. For through-the-wall radar applications, in addition to humans, there are only a finite number of objects that are commonly found inside rooms and behind walls, for example, chairs and tables of a few different sizes and possible shapes. As such, the underlying indoor imaging application is ideally suited for considering waveform design based on target signature exploitation.

Matched illumination waveform design is a signature exploitation technique in which waveform shaping is optimized to yield maximum signal-to-clutter-and-noise-ratio (SCNR) at the output of the receiver matched filter for optimal detection of targets with known impulse responses [2]-[3]. For target identification, the criterion is to design a waveform that maximizes the square of the Mahalanobis distance between the echoes from two targets [2]. Matched illumination was considered for the detection and identification of targets behind walls and in enclosed structures in [7] for single antenna monostatic operation. We presented a generalization of matched-illumination waveform design for through-the-wall target detection using a multistatic radar system in [8], wherein the system transmitters and receivers are spatially distributed over a wide area rather than being housed on the same physical platform. Such a scheme exploits the variations in the target impulse response as a function of the transmitter-to-target aspect angle and the transmitter-receiver bistatic angle for improved performance.

The objective of this paper is two-fold. First, we develop a vector formulation of the multistatic signal model in order to facilitate a discrete-time implementation of the matched illumination multistatic technique. Second, we extend the matched illumination waveform design for through-the-wall target identity discrimination. We analyze the performance of the proposed multistatic detection and identification system under both no-clutter and clutter-plus-noise scenarios and compare its performance to that of single antenna monostatic systems employing, respectively, an optimal matched illumination and a conventionally used chirp waveform.

2. SIGNAL MODEL

We consider a single stationary extended target inside a room with homogenous walls. Since the target remains within the same range gate and assumes the same impulse response, the set of transmitted waveforms need not be orthogonal, thereby allowing sequential use of the transmitters with simultaneous reception at multiple receivers. We assume coherent processing of the target returns at the different receivers. As such, a signal model can be developed based on single active transmitters.

2.1 Single Active Transmitter

Let the active transmitter be located at $\mathbf{x}_t = (x_t, y_t)$ and the M receivers be positioned at $\mathbf{x}_{rm} = (x_{rm}, y_{rm})$, $m = 1, 2, \ldots, M$, as shown in Fig. 1. If $z(t)$ is the energy-limited transmitted signal and $s_m(t)$ is the target return at the m-th receiver, then

$$s_m(t) = q_m(t) * z(t) \qquad (1)$$

where '$*$' denotes convolution and $q_m(t)$ is the combined wall/target impulse response corresponding to the m-th transmitter-receiver pair, and is given by

$$q_m(t) = u(t) * \xi_m(t) * u(-t) * \delta(t - \eta_m). \qquad (2)$$

In the above equation, $u(t)$ is the transmission impulse response of the wall, which is assumed to be known and independent of the transmitter and receiver locations. This is a reasonable assumption since, in general, the wall thickness is small compared to the typical antenna stand-off distance, which could be 10m or more from the wall. In this case, the differences in the path lengths through the wall as a function of antenna position are negligible. The deterministic function $\xi_m(t)$ is the known impulse response of the target corresponding to the m-th transmitter-receiver pair. Exact knowledge of the combined wall-target impulse response is required to implement matched illumination waveform design techniques. The case when the target impulse responses corresponding to the various transmitter-receiver pairs are not exactly known is discussed in a later section. The quantity η_m in (2) is the propagation delay measured from the transmitter to the target and then back to the m-th receiver and has contributions both from propagation through air and through the wall [9]. Since the target location and hence the delays η_m are not known beforehand, $q_m(t)$ should be assumed an unknown function. In order to overcome this issue, range gating is employed and the matched illumination waveform will be designed separately for each range gate within which the target could be present.

Let $w_{c,m}(t)$ represent the clutter response for the m-th transmitter-receiver pair and $n_m(t)$ be additive noise. Both the clutter and the noise are assumed to be stationary stochastic processes, which are independent of each other. The m-th received signal $r_m(t)$ is given by,

$$\begin{aligned} r_m(t) &= s_m(t) + c_m(t) + n_m(t) \\ c_m(t) &= w_{c,m}(t) * z(t) \end{aligned} \qquad (3)$$

where $c_m(t)$ is the signal dependent clutter return.

It is noted that in the above model, we have only considered the wall transmission impulse response. The wall reflections are assumed to have been either resolved from that of the target or mitigated using effective wall return removal techniques such as those recently proposed in [10]-[11]. In [10], the wall parameters are estimated and used to model the wall returns, which are then subtracted from the target scene data. The approach in [11] does not estimate the wall parameters and instead preprocesses the data by applying a filter in the spatial domain to notch the zero spatial frequency which corresponds to the approximately invariant signal returns from the wall at different antenna locations.

To facilitate simulation on a computer, we use a discrete-time formulation of the signal model. The transmitted signal $z(t)$ is given by N_z equally spaced time samples separated by an interval Δt, i.e., the transmitted signal vector is defined as $\mathbf{z} = [z_1, z_2, \ldots, z_{N_z}]^T$. Target impulse responses $\xi_m(t)$, $m = 1,2,\ldots,M$, can extend over different finite time durations. However, for simplicity of presentation, they are assumed to be of the same finite length. The combined wall/target impulse response $q_m(t)$ is sampled at the same rate as the transmitted signal to produce an $N_q \times 1$ impulse response vector $\mathbf{q}_m = [q_{m1}, q_{m2}, \ldots, q_{mN_q}]^T$ and the m-th received target return $s_m(t)$ is represented by the return signal vector, $\mathbf{s}_m = [s_1, s_2, \ldots, s_{N_s}]^T$, where $N_s = N_z + N_q - 1$. A convenient matrix representation of the m-th target return, free of noise and clutter, can be obtained following a similar formulation in [2] as

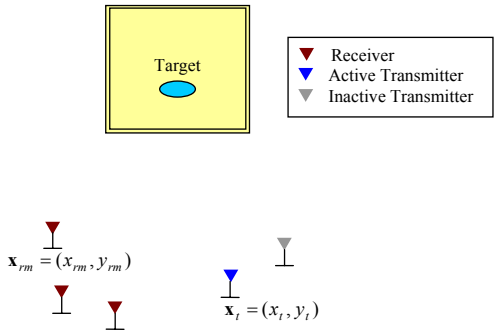

Figure 1 – Through-the-wall multistatic sensing scenario with a single active transmitter.

$$\mathbf{s}_m = \mathbf{Q}_m \mathbf{z} \qquad (4)$$

where the $N_s \times N_z$ combined wall/target convolution matrix $\mathbf{Q}_m$ is given by

$$\mathbf{Q}_m = \begin{bmatrix} q_{m1} & 0 & 0 & \cdots & 0 \\ q_{m2} & q_{m1} & 0 & \cdots & 0 \\ \vdots & \vdots & \vdots & \ddots & \vdots \\ q_{mN_q} & q_{m(N_q-1)} & \cdots & \cdots & q_{m(N_q-N_z)} \\ 0 & q_{mN_q} & \cdots & \cdots & q_{m(N_q-N_z+1)} \\ \vdots & \vdots & \vdots & \ddots & \vdots \\ 0 & 0 & \cdots & \cdots & q_{m(N_q-1)} \end{bmatrix} \qquad (5)$$

Likewise, by representing the clutter return and the noise by vectors of their respective temporal samples, the m-th received signal can be expressed in vector form as

$$\mathbf{r}_m = \mathbf{s}_m + \mathbf{c}_m + \mathbf{n}_m \qquad (6)$$

$$\mathbf{r}_m = [r_{m1}, r_{m2}, \ldots, r_{mN_s}]^T, \ \mathbf{c}_m = [c_{m1}, c_{m2}, \ldots, c_{mN_s}]^T$$

$$\mathbf{n}_m = [n_{m1}, n_{m2}, \ldots, n_{mN_s}]^T$$

We collect the received signals from the M receivers in an $MN_s \times 1$ vector $\mathbf{r}$

$$\mathbf{r} = \mathbf{Q}\mathbf{z} + \mathbf{c} + \mathbf{n} = \mathbf{s} + \mathbf{c} + \mathbf{n}$$

$$\mathbf{r} = \begin{bmatrix} \mathbf{r}_1 \\ \mathbf{r}_2 \\ \vdots \\ \mathbf{r}_M \end{bmatrix}, \ \mathbf{s} = \begin{bmatrix} \mathbf{s}_1 \\ \mathbf{s}_2 \\ \vdots \\ \mathbf{s}_M \end{bmatrix}, \ \mathbf{n} = \begin{bmatrix} \mathbf{n}_1 \\ \mathbf{n}_2 \\ \vdots \\ \mathbf{n}_M \end{bmatrix}, \ \mathbf{Q} = \begin{bmatrix} \mathbf{Q}_1 \\ \mathbf{Q}_2 \\ \vdots \\ \mathbf{Q}_M \end{bmatrix} \qquad (7)$$

2.2 Multiple Transmitters

Consider a multistatic through-the-wall radar system with L transmitters. When the l-th transmitter is active and

emits the signal $\mathbf{z}_l$, the $MN_s \times 1$ received signal vector $\mathbf{r}_{t_l}$ is given by (7), reproduced below with the introduction of the subscript l.

$$\mathbf{r}_{t_l} = \mathbf{Q}_{t_l}\mathbf{z}_l + \mathbf{c}_{t_l} + \mathbf{n}_{t_l} = \mathbf{s}_{t_l} + \mathbf{c}_{t_l} + \mathbf{n}_{t_l},\ l = 1,2,\ldots,L$$
$$\mathbf{r}_{t_l} = \begin{bmatrix} \mathbf{r}_{l1} \\ \mathbf{r}_{l2} \\ \vdots \\ \mathbf{r}_{lM} \end{bmatrix},\ \mathbf{s}_{t_l} = \begin{bmatrix} \mathbf{s}_{l1} \\ \mathbf{s}_{l2} \\ \vdots \\ \mathbf{s}_{lM} \end{bmatrix},\ \mathbf{n}_{t_l} = \begin{bmatrix} \mathbf{n}_{l1} \\ \mathbf{n}_{l2} \\ \vdots \\ \mathbf{n}_{lM} \end{bmatrix},\ \mathbf{Q}_{t_l} = \begin{bmatrix} \mathbf{Q}_{l1} \\ \mathbf{Q}_{l2} \\ \vdots \\ \mathbf{Q}_{lM} \end{bmatrix} \quad (8)$$

Note that we have assumed that each of the L transmitted signals has the same length N_z and the target impulse responses apparent to the LM transmitter-receiver pairs are all of length N_q. The values of N_z and N_q can be chosen based on their possible maximum values, consistent with system and target specifications and properties.

We combine the L received signals, obtained from the sequential use of the L transmitters, to form a tall vector $\mathbf{r}_{tot}$ of length LMN_s, given by

$$\mathbf{r}_{tot} = \mathbf{Q}_{tot}\mathbf{z}_{tot} + \mathbf{c}_{tot} + \mathbf{n}_{tot} = \mathbf{s}_{tot} + \mathbf{c}_{tot} + \mathbf{n}_{tot}$$
$$\mathbf{r}_{tot} = \begin{bmatrix} \mathbf{r}_{t_1} \\ \mathbf{r}_{t_2} \\ \vdots \\ \mathbf{r}_{t_L} \end{bmatrix},\ \mathbf{s}_{tot} = \begin{bmatrix} \mathbf{s}_{t_1} \\ \mathbf{s}_{t_2} \\ \vdots \\ \mathbf{s}_{t_L} \end{bmatrix},\ \mathbf{n}_{tot} = \begin{bmatrix} \mathbf{n}_{t_1} \\ \mathbf{n}_{t_2} \\ \vdots \\ \mathbf{n}_{t_L} \end{bmatrix} \quad (9)$$
$$\mathbf{Q}_{tot} = \begin{bmatrix} \mathbf{Q}_{t_1} & \mathbf{0} & \cdots & \mathbf{0} \\ \mathbf{0} & \mathbf{Q}_{t_2} & \cdots & \mathbf{0} \\ \vdots & \vdots & \ddots & \vdots \\ \mathbf{0} & \mathbf{0} & \cdots & \mathbf{Q}_{t_L} \end{bmatrix}$$

3. MATCHED ILLUMINATION WAVEFORM DESIGN

We assume that both the noise $\mathbf{n}_{tot}$ and the signal-dependent clutter return $\mathbf{c}_{tot}$ in (9) are independent zero-mean multivariate real Gaussian processes with known covariance matrices,

$$\mathbf{R}_n = E\{\mathbf{n}_{tot}\mathbf{n}_{tot}^T\} = \sigma^2\mathbf{I}_{LMN_s},\ \mathbf{R}_c = E\{\mathbf{c}_{tot}\mathbf{c}_{tot}^T\} \quad (10)$$

where $\mathbf{I}_{LMN_s}$ is an identity matrix of dimensions $LMN_s \times LMN_s$.

3.1. Optimum Detection Waveforms

The objective of the matched illumination detection waveform design is to find the transmitted signal vector $\mathbf{z}_{tot}$ that maximizes the SCNR at the output of the receiver matched filter, whose impulse response $\mathbf{b}_{match}$ is given by,

$$\mathbf{b}_{match} = (\mathbf{R}_c + \sigma^2\mathbf{I}_{LMN_s})^{-1}\mathbf{s}_{tot} \quad (11)$$

The SCNR at the output of the matched filter is given by

$$SCNR = \frac{\mathbf{b}_{match}^T\mathbf{s}_{tot}\mathbf{s}_{tot}^T\mathbf{b}_{match}}{(\mathbf{b}_{match}^T(\mathbf{R}_c + \sigma^2\mathbf{I}_{LMN_s})\mathbf{b}_{match})} \quad (12)$$

Using (11) and (12), the waveform design problem for optimal target detection can be formulated mathematically as,

$$\max_{\mathbf{z}_{tot}} \text{SCNR} = \max_{\mathbf{z}_{tot}} \mathbf{s}_{tot}^T(\mathbf{R}_c + \sigma_n^2\mathbf{I}_{LMN_s})^{-1}\mathbf{s}_{tot} \quad (13)$$

In the case of zero clutter, the SCNR simplifies to

$$\text{SCNR} = \frac{1}{\sigma_n^2}\mathbf{s}_{tot}^T\mathbf{s}_{tot} = \frac{1}{\sigma_n^2}\mathbf{z}_{tot}^T\mathbf{Q}_{tot}^T\mathbf{Q}_{tot}\mathbf{z}_{tot} \quad (14)$$

Exploiting the block-diagonal form of $\mathbf{Q}_{tot}$, we obtain

$$\text{SCNR} = \sum_{l=1}^{L}\mathbf{z}_l^T\mathbf{\Omega}_l\mathbf{z}_l, \qquad \mathbf{\Omega}_l = \frac{1}{\sigma^2}\mathbf{Q}_{t_l}^T\mathbf{Q}_{t_l} \quad (15)$$

Since the l-th term in the summation on the right hand side of SCNR in (15) depends only on the l-th transmission, it is clear that the original waveform design problem is equivalent to designing L individual waveforms $\mathbf{z}_1, \mathbf{z}_2, \ldots, \mathbf{z}_L$, such that

$$\max_{\mathbf{z}_l} \mathbf{z}_l^T\mathbf{\Omega}_l\mathbf{z}_l,\ \ l = 1,2,\ldots L \quad (16)$$

The solution $\mathbf{z}_l$ to the design problem of (16) is proportional to the eigenvector corresponding to the largest eigenvalue of $\mathbf{\Omega}_l$ [2].

On the other hand, when both signal-dependent clutter and noise are present and significant, the optimal waveform $\mathbf{z}_{tot}$ can be obtained iteratively, as discussed in [2].

3.2. Optimum Identification Waveforms

Maximizing the probability of correct identification is equivalent to the maximization of the Mahalanobis distance between the two target echoes [2],

$$\chi^2 = (\mathbf{s}_{tot,\alpha} - \mathbf{s}_{tot,\beta})^T(\mathbf{R}_c + \sigma_n^2\mathbf{I}_{LMN_s})^{-1}(\mathbf{s}_{tot,\alpha} - \mathbf{s}_{tot,\beta}) \quad (17)$$

where $\mathbf{s}_{tot,\alpha}$ and $\mathbf{s}_{tot,\beta}$ are the vectors corresponding to the echoes from targets α and β, respectively. Eq. (17) can be presented in terms of the combined wall/target convolution matrices as,

$$\chi^2 = \mathbf{z}_{tot}^T\mathbf{\Omega}_{\alpha,\beta}\mathbf{z}_{tot}$$
$$\mathbf{\Omega}_{\alpha,\beta} = (\mathbf{Q}_{tot,\alpha} - \mathbf{Q}_{tot,\beta})^T(\mathbf{R}_c + \sigma_n^2\mathbf{I}_{LMN_s})^{-1}(\mathbf{Q}_{tot,\alpha} - \mathbf{Q}_{tot,\beta}) \quad (18)$$

Similar to the no-clutter case for target detection, the optimum discriminating waveform is proportional to the eigenvector corresponding to the highest eigenvalue of $\mathbf{\Omega}_{\alpha,\beta}$. When the clutter is present in the scene, the optimal waveform is obtained via an iterative solution [2].

3.3. Ambiguity in Target Impulse Responses

Note that for a given range gate, the target impulse response at each receiver is a function of the transmitter-to-target aspect angle, which may not always be available when the target is behind walls. One simple way to overcome this problem is to cycle through all possible optimal matched-illumination waveforms for the target of interest given the multistatic sensor geometry. The SCNR varies as a function of the transmitter-to-target aspect angle, even when a corresponding optimal multistatic waveform is used or each orientation. Therefore, the transmitted waveform corresponding to the actual target orientation will provide the highest SCNR.

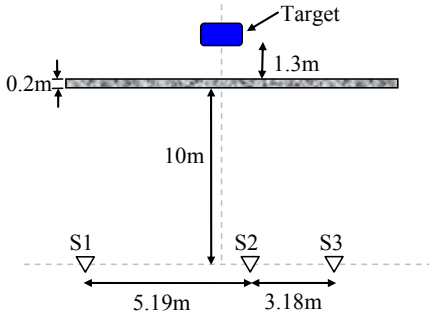

Figure 2 – Layout of the simulated scene.

4. SIMULATION RESULTS

A multistatic radar system, consisting of three sensors, was considered. Sensor S1 acts as a receiver, S2 is a transmitter, and S3 is a transceiver. The sensors are placed at a standoff distance of 10m from a 0.2in thick solid concrete wall with $\varepsilon = 7.6$ and $\sigma = 0.05$ S/m, as depicted in Fig. 2. The target is located 1.3m behind the wall. A wooden table and the model of a human, shown in Fig. 3, were considered as targets. The particular human model used is the "High Fidelity Frozen Male Body" by Remcom Inc. The human's phantom consists of 23 different tissue types, each with its own dielectric properties. The model is optimized for numerical computations and occupies only 128 MB of RAM [12].

Since the optimal waveform design involves target impulse responses, free-space simulations were first carried out using a commercial electromagnetic simulator XFDTD® by Remcom for computing the impulse responses of the targets apparent to each transmitter/receiver pair. It was assumed that both the transmitter and the receiver are located in the far-field of the target. Each target was probed by a vertically polarized modulated Gaussian pulse, covering the 1-8 GHz frequency band with almost uniform energy over 1-3 GHz. For each transmitter/receiver bistatic angle, the corresponding target impulse response $\boldsymbol{\xi}$ was obtained as the least squares solution $\boldsymbol{\xi} = (\mathbf{Z}^T\mathbf{Z})^{-1}\mathbf{Z}^T\mathbf{s}$, where $\mathbf{Z}$ is a convolution matrix, identical in structure to (5), containing the incident modulated Gaussian waveform, and $\mathbf{s}$ is the target return vector [7]. The transmission impulse response of the wall was similarly computed. Since XFDTD® produced results for a far-field scenario with plane wave excitation, the combined wall/target impulse responses were preprocessed to reflect the multistatic operation.

Optimal matched illumination detection waveforms were constructed for the human for the zero clutter case. A range gate of 18.5 ns, centered at the target, was used. The SCNR corresponding to the multistatic radar system using the optimal waveforms is provided in Table I. For comparison, the optimal matched illumination waveform corresponding to monostatic operation from the transceiver, was also obtained and the corresponding SCNR is given in Table I. In order to compare the performance of the different waveforms, we used the same total transmit power and identical noise variance of 0.001. We note that the multistatic system of the human apparent to the two receivers (S3 and S1) with

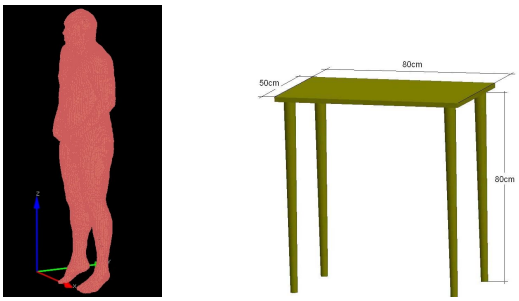

(a) (b)

Figure 3. (a) High Fidelity Frozen Human, (b) Wooden table.

Table I. SCNR at matched filter output for the human.

Waveform	SCNR (dB)	
	Monostatic Operation	Multistatic Operation
Optimal	-7.7216	0.7260
Chirp	-14.8094	-10.6277

transmitter S3 active, and the frequency response of the optimal multistatic waveform transmitted from S3. It is clear from the figure that the optimal waveform places its energy in a narrow frequency band that jointly resonates the wall and the target. The optimal waveform corresponding to transmitter S3 is plotted in Fig. 5(a).

The output SCNRs corresponding to the optimal transmitted waveforms for monostatic and multistatic operations were also compared to those of chirp waveforms of the same energy and respective durations. The SCNRs corresponding to the chirp waveforms for the human are provided in Table I. It is evident that the optimal waveforms significantly outperform the chirp signal for both monostatic and multistatic operations. In fact, for the target and scene layout considered, the optimal monostatic waveform outperforms the multistatic radar employing chirp waveforms.

For the case of non-zero clutter, we have designed the optimum multistatic waveforms for the human using the iterative algorithm presented in [2]. The clutter and the noise are assumed to be of independent samples. The clutter-to-noise ratio (CNR) was first set to -10 dB and then to 10dB. Table II provides the SCNR at the output of the matched filter due to three different waveforms, namely, the optimum transmitted waveform for clutter and noise, the optimum waveform for noise only case, and a chirp waveform, all of the same duration and energy. For CNR of -10 dB, we observe that the optimized waveform obtained via the iterative technique provides better detection in the presence of clutter, though the overall SCNR improvement compared to the noise only case has degraded. On the other hand, when the CNR is 10 dB, all transmission waveforms yield similar SCNR. This is in compliance with the degenerate case of significant clutter, described in [2], wherein all transmission waveforms yield identical SCNR. The optimal waveform corresponding to transmitter S3 for CNR=-10 dB is plotted in Fig. 5(b). We also designed the optimal multistatic waveform for detection of human in the presence of noise and with the wooden table as a source of clutter. Since the table frequency response (not shown) does not have significant energy beyond 5 GHz, the corresponding waveform was

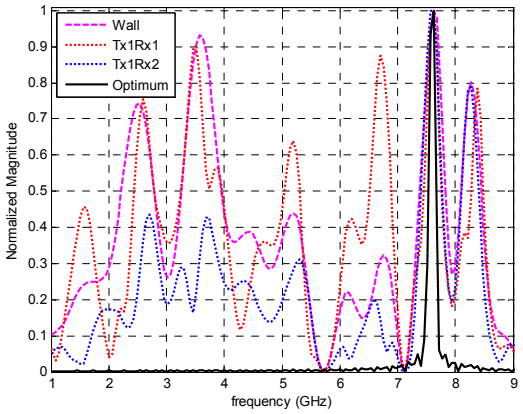

Figure 4. Normalized Magnitude Spectra with S3 transmitting.

Table II. Multistatic SCNR at matched filter output for the human.

Waveform	Multistatic SCNR (dB)	
	CNR= -10 dB	CNR=10 dB
Optimal – Clutter and Noise	-24.9107	-42.7754
Optimal – Noise only	-25.9141	-43.2472
Chirp	-29.6381	-42.1243

similar to the noise-only multistatic waveform for human detection.

In order to evaluate the performance of optimal waveforms for discrimination between different targets of interest, i.e., the table and the human, we examined the Mahalanobis distances between the targets' echoes under both monostatic and multistatic operation in the presence of noise for different transmitted signals. We compare the optimal discrimination waveforms, a chirp waveform, and the optimal detection waveforms for the human and the table. The results, provided in Table III, show the advantage of using the optimal multistatic discrimination waveforms.

5. CONCLUSIONS

In this paper, we presented a generalization of the matched illumination based waveform design for through-the-wall radar operation using a multistatic radar system for improved detection and identity discrimination of stationary targets. The slowly moving and stationary nature of the indoor targets permits sequential use of the transmitters, rendering the use of orthogonal waveforms unnecessary. Proof of concept was provided using electromagnetic modeled data for a human and a wooden table behind a solid concrete wall. The two cases of noise-only and clutter-plus-noise were analyzed. It was assumed that the target signal returns to a transmitted waveform can be coherently processed at the different receivers. Performance of the optimal multistatic waveform was shown to be superior to that of the optimum waveform for single antenna monostatic operation as well as a conventionally used chirp waveform.

ACKNOWLEDGEMENT

This work was supported by ONR under grant N00014-07-1-0043.

Table III. Mahalanobis distance for multistatic operation.

Waveform	Mahalanobis distance (dB)	
	Monostatic Operation	Multistatic Operation
Optimal	-21.7629	7.2545
Optimal human detection	-36.888	6.4546
Optimal table detection	-21.7623	6.9482
Chirp	-34.1954	-5.003

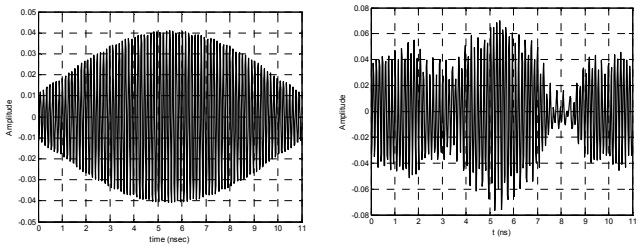

(a) (b)

Figure 5: Optimal waveform with S3 transmitting (a) noise only, (b) CNR=-10dB.

REFERENCES

[1] J. A. Malas and K. M. Pasala, "Radar signature analysis using information theory," in *IEEE Radar Conf.*, Pisa, Italy, May 2008.

[2] D. A. Garren, et. al, "Enhanced target detection and identification via optimised radar transmission pulse shape," *IEE Proc.-Radar, Sonar Navig.*, vol. 148, No. 3, pp. 130-138, Jun. 2001.

[3] D. T. Gjessing, *Target adaptive matched illumination RADAR: Principles and applications*, IEE Electromagnetic Waves Series 22, Peter Peregrinus Ltd., London, UK, 1986.

[4] *Journal of the Franklin Institute*, Special Issue on 'Advances in Indoor Radar Imaging,' vol. 345, no. 6, Sep. 2008.

[5] E. F. Greneker, "RADAR flashlight for through-the-wall detection of humans", in *Proc. SPIE*, vol. 3375, Apr. 1998, pp. 280-285.

[6] M. Pieraccini, et. al, "Detection of Breathing and Heartbeat Through Snow Using a Microwave Transceiver," *IEEE Geosci. Remote Sens. Lett.*, vol. 5, no. 1, pp. 57-59, 2008.

[7] H. Estephan, M. Amin, and K. Yemelyanov, "Waveform design for through-the-wall radar imaging applications," in *Proc. SPIE*, vol. 6943, Mar. 2008, pp.

[8] F. Ahmad, M. Amin, H. Estephan, "Multistatic waveform design for seeing through the wall," in *Proc. Waveform Design and Diversity Conf.*, Orlando, FL, Feb 2009.

[9] F. Ahmad and M. G. Amin, "Noncoherent approach to through-the-wall target localization," *IEEE Trans. Aerosp. Electron. Syst.*, vol. 42, issue 4, pp. 1405-1419, Oct. 2006.

[10] M. Dehmollaian and K. Sarabandi, "Refocusing through building walls using synthetic aperture radar," *IEEE Trans. Geosci. Remote Sens.*, vol. 46, no. 6, pp. 1589–1599, Jun. 2008.

[11] Y. Yoon and M. Amin, "Spatial filtering for wall-clutter mitigation in through-the-wall radar imaging," *IEEE Trans. Geosci. Remote Sens.*, under review.

[12] Available: http://www.remcom.com/xfdtd/optional-modules/ biological-meshes.html.